Fatigue Behavior of Noncomposite Reinforced Concrete Bridge Deck Models

MICHAEL F. PETROU, PHILIP C. PERDIKARIS, AND AIDONG WANG

The fatigue performance of the AASHTO and Ontario Highway Bridge Design Code (OHBDC) designs for noncomposite reinforced concrete bridge decks was studied on the basis of tests conducted on small-scale physical models. The type of fatigue loading has a profound influence on the fatigue behavior of the decks. Under a moving constant wheel-load, the initial two-way deck slab action changes to a one-way slab action, whereas under a stationary pulsating load the two-way action is maintained until failure. The bridge decks subjected to a stationary pulsating load exhibited a flexural radial cracking; those under a moving constant wheel-load exhibited a flexural gridlike pattern similar to the grid of the bottom steel layer. For a given applied fatigue load level, the decks subjected to a stationary pulsating loading regime exhibited higher fatigue life than those subjected to a moving constant wheel-load. On the basis of an exponential curve fit of the fatigue data in this study, the 2.5 million load cycle deck fatigue strength under a stationary pulsating load ranges between 0.47 and 0.54 P_u (safety factor against a 2.5 million load cycle fatigue failure of 5 to 12), where P_u is the measured static ultimate strength. On the other hand, the 2.5 million wheel-load passage deck fatigue strength under a moving constant wheel-load is estimated to be between 0.21 and 0.28 P_u (safety factor of 3 to 4). If the efficiency of the deck fatigue design is determined by the number of wheel-load passages on the deck at a given moving wheel-load level ratio (P/P_u) without deck failure, the OHBDC deck design appears to be more efficient than the AASHTO design.

Current AASHTO Code provisions (*1*) require concrete bridge decks to be orthotropically reinforced. They are designed as beams transverse to the traffic direction supported on the steel girders and carrying the traffic loads in flexure. On the basis of the AASHTO deck design, a concrete deck of a steel stringer bridge is reinforced for flexure transversely to the steel girders with a steel ratio of about 0.7 percent in each top and bottom steel layer and longitudinally (traffic direction) with a steel ratio of about 0.35 percent for each steel layer. This approach does not take into account the two-way slab action in the bridge deck and the enhancement of its flexural and shear ultimate strength caused by membrane compressive action (*2–9*).

Since the early 1960s, the lack of adequate understanding of the fatigue behavior of concrete deck slabs has started to be alarming in view of the ever-growing intensity of traffic and the serious deterioration of the highway bridge system. It is becoming increasingly important to determine the effect of moving wheel-loads on the fatigue structural response of reinforced concrete decks, including the cracking pattern and failure mode. Extensive studies on the failure mechanism of small-scale reinforced concrete bridge deck models subjected to static and stationary pulsating concentrated loads were performed at Queen's University at Kingston, Ontario, Canada (*8–11*), University of Petroleum and Minerals, Dhahran, Saudi Arabia (*2*), and the University of Texas at Austin (*12,13*) and Case Western Reserve University (*3–7,14,15*) in the United States. On the basis of the results of the full-scale and small-scale tests performed under static and stationary pulsating loads at Queen's University, an "isotropic" steel reinforcement pattern with equal amounts of steel reinforcement of 0.3 percent in the transverse and longitudinal directions (each top and bottom steel layer) was adopted in the Ontario Highway Bridge Design Code [OHBDC, (*16*)]. This steel reinforcement arrangement reduced the reinforcement content in the deck by up to 60 percent, considerably increasing the durability of such decks because of better protection of the top steel layer and undoubtedly lowering their construction and maintenance cost.

Tests performed in Japan (*17,18*) showed that the flexural and shear rigidity of the deck slab under a "stepwise" moving wheel-load are dramatically reduced compared with that under a stationary pulsating load. One passage of a stepwise moving wheel-load consists of applying a single concentrated load in sequence at a set of preselected equally spaced points on the deck along the loading path. A loading setup was designed and constructed at Case Western Reserve University to simulate a moving constant wheel-load in an extensive experimental program funded by the Ohio Department of Transportation (ODOT) and FHWA (*3,4,14*). Fatigue studies under moving load were also performed in Japan at Osaka City University (*19,20*). The preliminary experimental results by Perdikaris and Beim (*3,14*), Perdikaris et al. (*4*), and Sonoda et al. (*20*) indicated a substantial reduction in the bridge deck's fatigue life if the decks were subjected to a moving wheel-load instead of a stationary pulsating load. In the former research study (*3,4,14*), "isotropically" reinforced OHBDC decks and "orthotropically" reinforced AASHTO decks were fatigued under moving wheel-loads equal to 60 percent of their static ultimate strength to determine their fatigue strength under overload conditions. The OHBDC decks exhibited longer fatigue lives than the AASHTO decks under this high fatigue load level.

The objective of this paper is to present selected results on the fatigue response of noncomposite reinforced concrete bridge deck models and compare the fatigue performance of the AASHTO and OHBDC deck design.

EXPERIMENTAL SETUP

Full-Scale Bridge Structure

The prototype highway bridge structure represents a simply supported noncomposite reinforced concrete deck-on-steel girder bridge with a span of 15.24 m (50 ft) and a thickness of 21.6 cm

M. F. Petrou, Department of Civil Engineering, University of South Carolina, Columbia, S.C. 29208. P. C. Perdikaris and A. Wang, Department of Civil Engineering, Case Western Reserve University, Cleveland, Ohio 44106.

(8.5 in.). The deck slab is supported on four W36 × 150 steel girders spaced at 2.13 or 3.05 m (7 or 10 ft). Two deck designs are studied in this paper. According to the AASHTO design provisions, the deck slab is assumed to be orthotropically reinforced with No. 6 Grade 60 deformed steel rebars [d = 19 mm (0.75 in.)]. This orthotropic flexural steel reinforcing arrangement (AASHTO) corresponds to steel ratios of about 0.7 and 0.35 percent in each steel layer. The isotropic steel reinforcing pattern (OHBDC), on the other hand, consists of transverse and longitudinal flexural steel ratio of 0.3 percent for each top and bottom steel layer.

Bridge Deck Model (1/6.6 Scale)

The full-scale W36 × 150 steel girders were modeled by M6 × 4.4 steel I-beams. Diagonally braced L-shaped steel struts sized 25.4 × 12.7 × 3.2 mm (1 × ½ × ⅛ in.) were used to model the transverse bridge diaphragms between adjacent steel girders, as shown in Figure 1. The deck slab thickness is 36 mm (1.4 in.). The deformed steel wire used as model steel reinforcement has a nominal diameter of 2.8 mm (0.11 in.) and a cross-sectional area of 6.1 mm^2 (0.0095 in.^{2}). The dimensions of the model bridge specimen for a 2.13-m (7-ft) full-scale girder spacing are indicated in Figure 1. The forms for the concrete deck specimens were made of Plexiglas, which is an adequately stiff, lightweight, and reusable material. No steel shear studs were used because only noncomposite deck behavior was studied.

Each deck specimen was divided transversely into three "lanes." Each lane, which is the part of the deck between two adjacent steel girders with a length equal to the deck's length and a width equal to the girder spacing, is labeled east (E), center (C), and west (W) and divided longitudinally into three regions labeled north (N), center (C), and south (S), as indicated in Figure 1. Thus, nine deck regions (SW, CW, NW, SC, CC, NC, SE, CE, and NE) were tested under a static or a stationary pulsating load and three lanes were tested under a moving wheel-load.

For the OHBDC deck models, the steel reinforcement wires were spaced at about 56 mm (2.2 in.) in both directions (top and bottom steel layer). In the case of the AASHTO deck models, the deformed steel wires were spaced transversely and longitudinally at about 24 and 48 mm (0.94 and 1.88 in.), respectively. The concrete cover was about 4 mm (0.15 in.) for the top steel layer (longitudinal) and 8 mm (0.3 in.) for the bottom steel layer (transverse).

Materials

The prototype material behavior of concrete and steel reinforcement is properly modeled (*21*) by scaling the aggregates for the model concrete and using deformed wire for the model reinforcement. The measured average uniaxial cylinder concrete compressive strength is about 44 MPa (6,400 psi), as indicated in Table 1. The measured average concrete tensile strength based on splitting tension cylinder tests is 5.7 MPa (830 psi) for the cylinders 5.1 × 10.2 cm (2 × 4 in.) and 4.5 MPa (650 psi) for the cylinders 10.2 × 20.4 cm (4 × 8 in.).

The assumed full-scale steel reinforcement of No. 6 Grade 60 deformed steel bars [d = 19 mm (0.75 in.)] with a yield strength of 413 MPa (60 ksi) and modulus of elasticity of 199,810 MPa (29,000 ksi) is modeled with D-1 steel wire deformed in the models laboratory. The deformed steel wire was annealed for 2 hr at 580°C (1,076°F) to lower its yield strength to the desired level of about 413 MPa (60 ksi) and increase its ductility (strain of about 20 percent at failure). The nominal diameter of the model steel reinforcement is about 2.8 mm (0.11 in.).

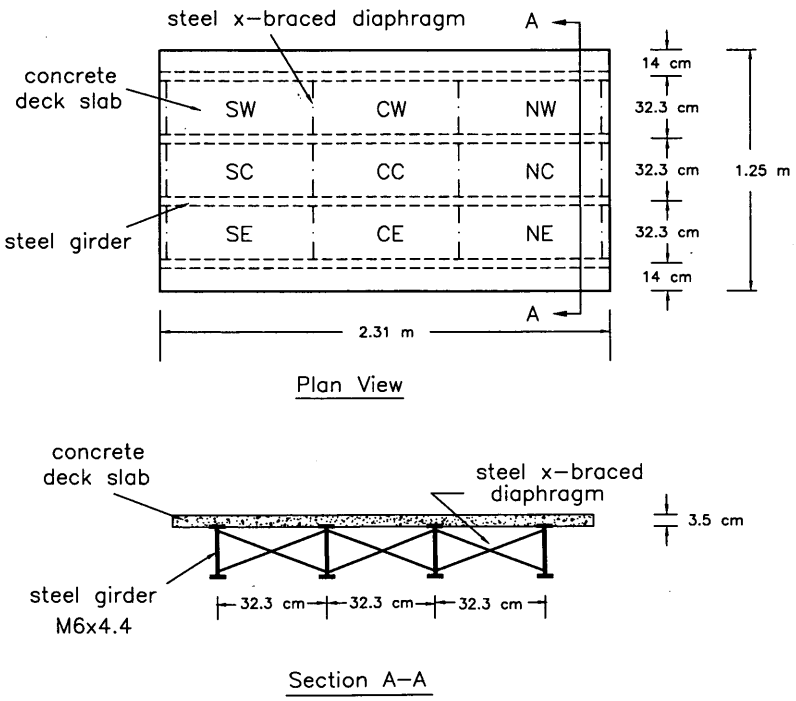

FIGURE 1 Dimensions of the 1/6.6-scale bridge deck model with a prototype girder spacing of 2.13 m (1 m = 3.28 ft and 1 cm = 0.394 in.).

TABLE 1 Experimental Program for 1/6.6-Scale Bridge Deck Models (1 m = 3.28 ft, 1 cm = 0.394 in., and 1 MPa = 0.145 ksi).

Deck Specimen	Full-scale Girder Spacing (m)	Flexural Steel Reinforcement Pattern	Average Compressive Strength, f_c' (MPa)		Number of Tests		
			5.1x10.2 cm Cylinder	10.2x20.4 cm Cylinder	Static Load	Pulsating Load	Moving Load
BI3-7SP(1)	2.1	Isotropic[a]	-	-	5	4	-
BI3-7SPM(2)			-	-	2	1	2
BI3-7M(3)			41.8	-	-	-	4
BI3-10SP(1)	3.0	Isotropic	50.0	48.0	6	3	-
BI3-10M(2)			49.5	48.0	-	-	3
BI3-10SPM(3)			42.4	44.6	1	2	2
BI3-10PM(4)			40.1	40.1	-	3	2
BO-7SPM(1)	2.1	Orthotropic[b]	45.6	45.9	2	2	2
BO-7PM(2)			39.7	37.1	-	3	2
BO-10SP(1)	3.0	Orthotropic	48.3	41.1	6	3	-
BO-10M(2)			-	-	-	-	3
BO-10M(3)			42.2	-	-	-	3
BO-10PM(4)			39.5	-	-	2	3

Notes:
[a]Isotropic: ρ_l =0.003 (longitudinal) and ρ_t=0.003 (transverse); top and bottom-Ontario design.
[b]Orthotropic: ρ_l =0.0035 (longitudinal) and ρ_t=0.007 (transverse); top and bottom-AASHTO design.

Loading Setup

The loading setup used for the static and stationary pulsating load tests is a steel reaction frame bolted to the floor and a 222.5-kN (50-kips) hydraulic actuator with a maximum stroke of 15.2 cm (6 in.). The wheel-load is applied to the deck specimen at specific locations through a rubber pad 9.5 mm (3/8 in.) thick bonded to a steel plate 91.4 × 38.1 × 9.5 mm (3.6 × 1.5 × 3/8 in.), which models a representative full-scale 61 × 25.4 cm (24 × 10 in.) contact area of a pair of truck tires. The stationary pulsating load tests were performed using load control at an average frequency of 7 Hz. The loading frequency of 7 Hz for the 1/6.6-scale models corresponds to a frequency of about 1 Hz for the full-scale bridge deck structure. A truck traveling speed of 88.5 km/hr (55 mph) for a 15.24-m (50-ft) span bridge corresponds to a loading frequency of about 1.7 Hz for any point of the deck. The pulsating load varied sinusoidally with a minimum load level of about 2.2 kN (500 lb) and a maximum load level equal to that selected for each test.

A moving constant wheel-load setup was developed in the first phase of this study (*3,4,14*). As shown in Figure 2, it consists of a moving steel trailer bolted to a hydraulic jack that applies a constant wheel-load to the deck specimen through a steel reaction frame attached to the floor. The wheel-load is applied to the deck through a steel wheel coated with polyurethane attached to the bottom of the jack by a steel yoke. A pressure accumulator enables the applied load to be controlled within a variation of about ±3 percent. The hydraulic actuator with a 15.2-cm (6-in.) stroke has a capacity of 133.5 kN (30,000 lb). The jack-wheel assembly, powered by a hydraulic motor, moves back and forth at a maximum speed of about 61 cm/sec or 2.2 km/hr (2 ft/sec or 1.4 mph). Similitude requirements demand the traffic speed in the full-scale deck to be the same as in the models. Thus, because the model speed is far lower than a reasonable "design" speed of 88.5 km/hr (55 mph), the results of this study on the fatigue response under a constant moving wheel-load do not include any possible dynamic effects present at normal traffic speeds.

Experimental Program: Parameters, Instrumentation

The experimental program discussed in this paper is shown in Table 1. The bridge deck models were subjected to concentrated static load, stationary pulsating, and moving constant wheel-load (*22,23*). Only the experimental results on the fatigue behavior (cracking patterns and failure modes) for the 1/6.6-scale bridge deck models (reinforced according to AASHTO and OHBDC specifications) under stationary pulsating and moving constant wheel-load are discussed. Full-scale girder spacings of 2.13 and 3.05 m (7 and 10 ft) were considered. The boundary conditions of the deck, which affect the deck restraint level, varied from "simply supported" (bridge deck panel models, which are not presented here) to "continuous" (central region of the bridge deck models).

The instrumentation used for the tests included displacement transducers (DCDTs), load cells, and strain gauges. For acquiring

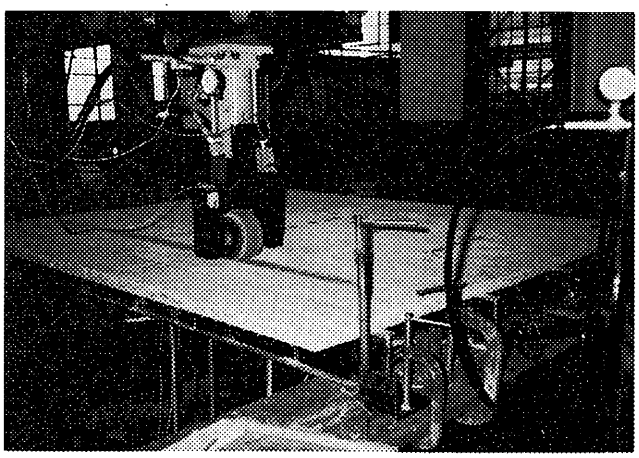

FIGURE 2 Moving constant wheel-load setup.

the global structural response of the bridge deck and assessing the induced static and fatigue damage in the concrete deck slab, three DCDTs were used to measure the vertical displacement of two adjacent steel girders and the deck midway between the two girders at a specified section along the deck. Epoxy-bonded electrical resistance foil-backed strain gauges were used to measure the axial strains in the steel reinforcement at selected locations of the top and bottom steel layer, flexural strains in the steel girders, and strains on the concrete deck surface.

DISCUSSION OF EXPERIMENTAL RESULTS

Effect of Load Level

The log of the number of load cycles to failure under stationary pulsating load, $\log N_{cf}$, and the log of the number of wheel-load passages to failure under moving constant wheel-load, $\log N_{pf}$, are presented as a function of the applied model load and the ratio of applied model load to deck static ultimate strength in Figures 3 through 6. The fatigue data correspond to a punching deck failure at a specific deck region subjected to a given stationary pulsating or moving constant wheel-load level. In the case of the moving wheel-load fatigue tests, a deck lane will fail sequentially at various locations, whereas the test is usually continued until a punching deck failure eventually occurs in the vicinity of midspan (usually the second or third consecutive failure). This means that for a given moving wheel-load fatigue level there could be a maximum of three fatigue strength data points.

Stationary Pulsating Load

For unrealistically high stationary pulsating concentrated load levels that are more than 60 percent of the deck's measured static ultimate strength, P_u, the deck fatigue strength appears to be less than 10,000 load cycles. The primary deck failure mode at this high fatigue load level is punching but for a load level lower than 0.6 P_u, the primary fatigue failure in the deck occurs in a combined flexural-punching mode. Usually the lower the applied load level the more primary the flexural failure. For bridge decks subjected to static loads or high

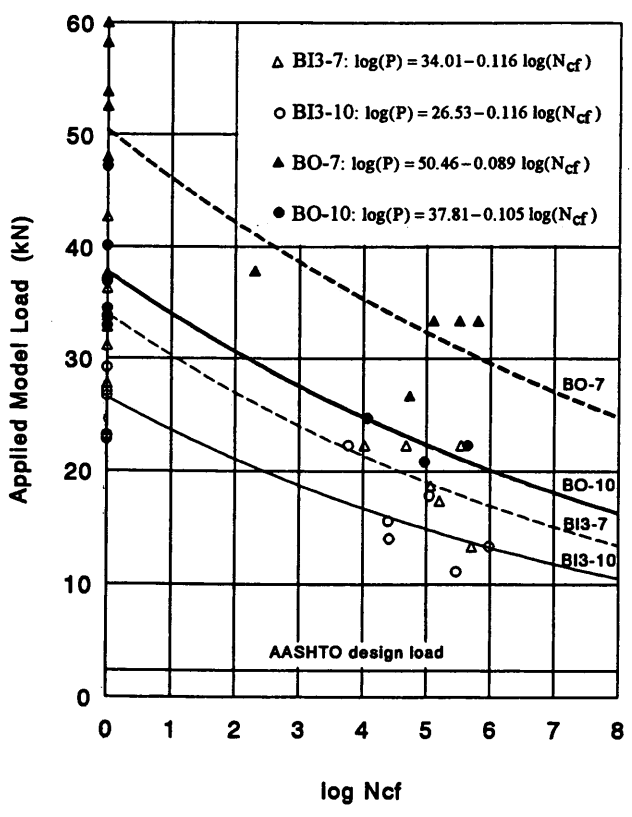

FIGURE 3 *S-N* fatigue curves under stationary pulsating load in terms of the applied load level versus log N_{cf} (1 kN = 225 lb).

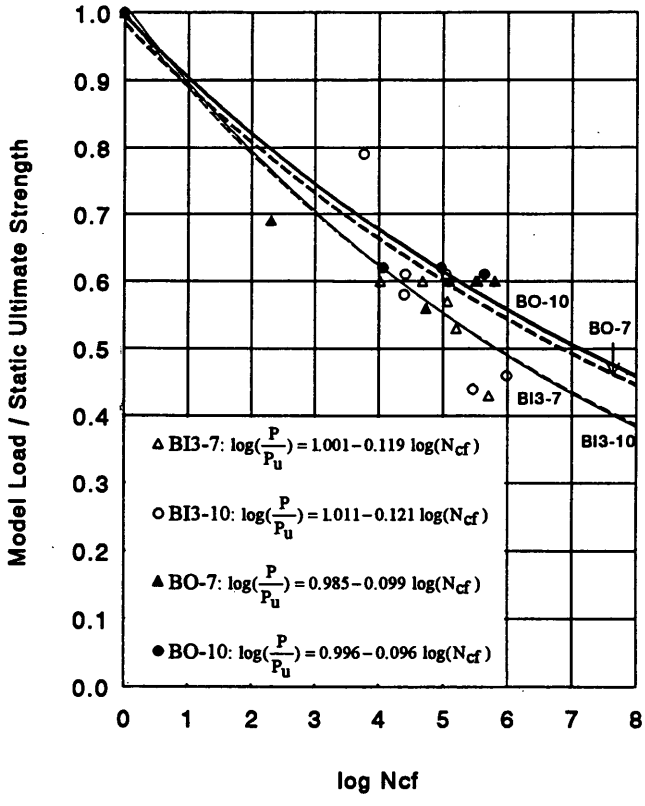

FIGURE 4 *S-N* fatigue curves under stationary pulsating load in terms of the ratio of applied load to static ultimate strength versus log N_{cf}.

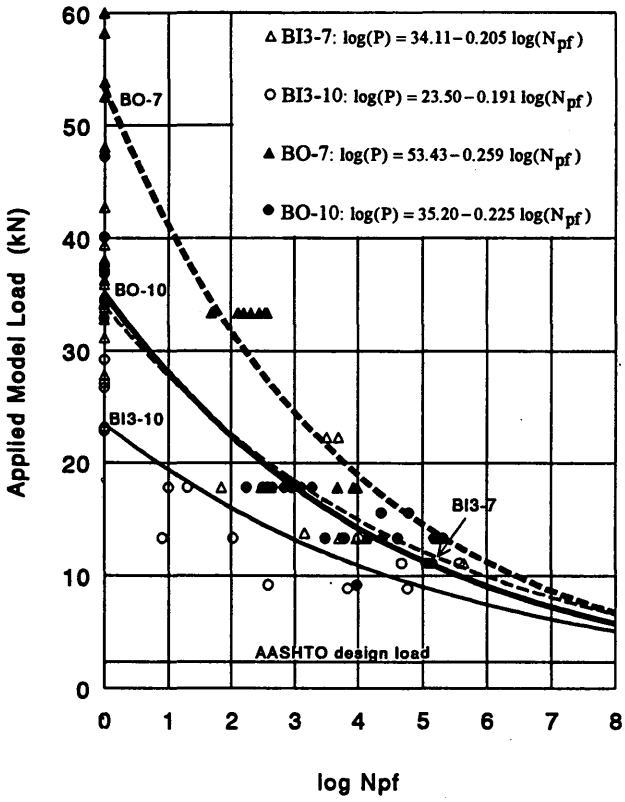

FIGURE 5 *S-N* fatigue curves under moving constant wheel-load in terms of the applied load level versus log N_{pf} (1 kN = 225 lb).

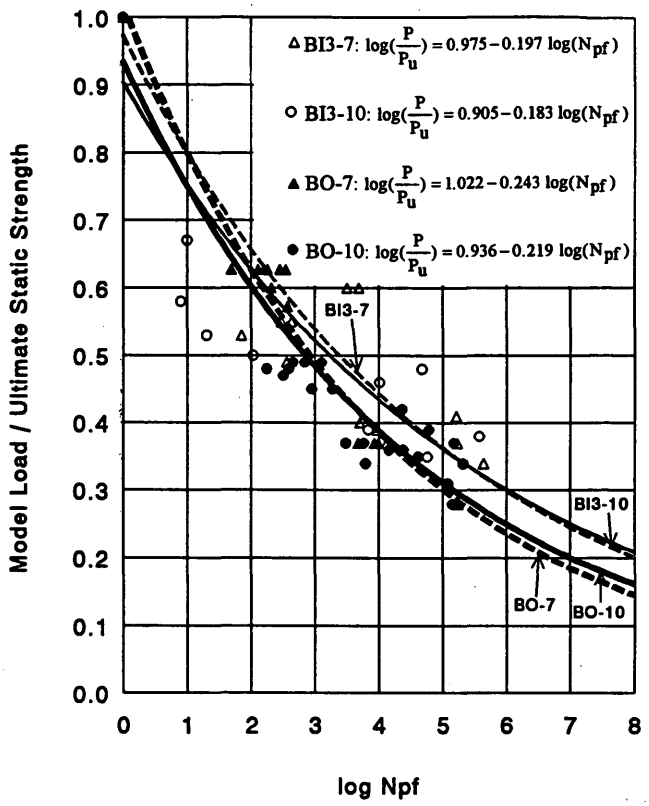

FIGURE 6 *S-N* fatigue curves under moving constant wheel-load in terms of the ratio of applied load to static ultimate strength versus log N_{pf}.

fatigue load levels, failure occurs suddenly without yielding of the steel reinforcement beyond the loaded area, whereas for bridge decks under low fatigue load level extensive yielding of the steel reinforcement is necessary for failure to occur. Further discussion of this behavior will be presented in another paper.

The estimated fatigue strength values in terms of the static ultimate strength and maximum measured AASHTO deck static ultimate strength ratios are presented in Table 2 for 1,000, 2.5 million, and 100 million load cycles. The safety factors against fatigue failure after 2.5 million load cycles presented in Table 2 are based on a model design load of 2.3 kN (525 lb). The model design load is determined by dividing the full-scale AASHTO design load of 92.6 kN (20.8 kips), including an impact factor of 1.3, by S_l^2, where S_l is the length scale factor. The fatigue strength levels are estimated on the basis of the following expression:

$$\log P \text{ or } \log\left(\frac{P}{P_u}\right) = A + B \cdot \log N_{cf} \qquad (1)$$

where A and B are constants estimated by the least-squares method (see Figures 3 and 4). The exponential curve fitting of the experimental data points presented in Figure 3 (P versus log N_{cf}) is based on Equation 1 and corresponds to correlation coefficients between 0.71 and 0.86. In Figure 4 (P/P_u versus log N_{cf}), the exponential curve fitting of the data points corresponds to correlation coefficients between 0.92 and 0.98.

The predicted bridge deck fatigue strength at 2.5 and 100 million load cycles under stationary pulsating concentrated load ranges from 0.27 to 0.48 P_a and 0.22 to 0.41 P_a, respectively, where P_a is the largest measured AASHTO deck static ultimate strength. The predicted safety factor against fatigue failure in the deck under a stationary pulsating load for the 2.5 million load cycle limit is about 5 to 7 for the OHBDC design and 8 to 12 for the AASHTO design (see Table 2). The predicted deck fatigue strength at 2.5 million load cycles expressed in terms of the deck's static ultimate strength is at least twice the cracking load level and ranges between 0.47 and 0.54 P_u, as indicated in Figure 4 and Table 2. This value is close to the generally accepted 2.5 million load cycle fatigue strength of plain concrete and consistent with that of 0.5 P_u according to Batchelor et al. (*11*) and slightly lower than 0.6 P_u according to Azad et al. (*2*). The AASHTO decks exhibited higher fatigue strengths than the OHBDC decks when they were subjected to the same load level, the same ratio of load to static ultimate strength, or the same ratio of load to maximum measured AASHTO static ultimate strength.

On the basis of steel reinforcement strain measurements (*22,23*) under a stationary pulsating load, there is a two-way action in the deck slabs. The observed cracking pattern is similar to that produced by a static concentrated load. On the top deck surface, the damage around the loaded area is minor. A fan-shaped pattern of radial positive cracks emanating from the load application point is observed at the bottom deck surface under the loaded region. The radial bottom flexural cracks open and close as the applied pulsating load varies from the minimum to the maximum value. The reinforcing flexural bars blunt the cracks, and larger deformations in the flexural steel reinforcement are required for the cracks to propagate in the deck. As soon as the steel reinforcement yields, the

TABLE 2 Predicted Fatigue Strength of Reinforced Concrete Bridge Decks Based on Exponential Curve Fitting of Experimental Data

Specimen	Predicted Fatigue Strength (P/P_a and P/P_u)												Safety Factor	
	Stationary Pulsating Load (number of load cycles, N_{cf})						Moving Constant Wheel-load (number of wheel passages, N_{pf})							
	1,000		2,500,000		100,000,000		1,000		2,500,000		100,000,000		Pulsating	Moving
	P/P_a	P/P_u	P/P_a	P/P_u	P/P_a	P/P_u	P/P_a	P/P_u	P/P_a	P/P_u	P/P_a	P/P_u	N_{cf}=2.5 mil.	N_{pf}=2.5 mil.
BO-7	0.64	0.73	0.48	0.52	0.41	0.45	0.41	0.49	0.17	0.21	0.11	0.14	12.2	4.4
BO-10	0.58	0.74	0.41	0.54	0.35	0.46	0.38	0.48	0.18	0.23	0.12	0.16	8.3	3.6
BI3-7	0.40	0.70	0.27	0.47	0.22	0.39	0.31	0.54	0.15	0.28	0.11	0.20	6.9	3.9
BI3-10	0.40	0.70	0.27	0.47	0.22	0.38	0.28	0.52	0.15	0.28	0.11	0.21	5.4	3.0

Notes:
P = Applied load.
P_a = Largest static ultimate strength of "AASHTO" decks.
P_u = Static ultimate strength.

cracks propagate rapidly, and the cumulative damage of the deck increases. This explanation is supported by the fact that yielding of the steel reinforcement underneath the loaded area occurs at a load level of 0.4 to 0.6 P_u, which is similar to the 2.5 million load cycle fatigue strength range under a stationary pulsating load. At this point, the total and the per-cycle (static "load-unload" cycles) peak deck deflection versus the number of load cycles increase rapidly. After the deck damage reaches a critical level, the deck collapses.

Moving Constant Wheel-Load

The deck fatigue life is extremely short at less than 10 wheel-load passages under wheel-load levels higher than 0.7 P_u, as shown in Figure 6. The fatigue failure in the deck is sudden and is caused by punching shear. For lower wheel-load levels, flexure becomes the primary failure mode. The fatigue strength of the decks subjected to moving wheel-loads is consistently lower than that under stationary pulsating loads of the same magnitude or the same ratio of load to static ultimate strength. Because of time constraints, the fatigue tests performed under a moving load resulted in far fewer than 2.5 million wheel-load passages to failure. The highest number of wheel-load passages to failure recorded was 439,204 for the west-lane deck of B13-7SPM(3) subjected to a moving constant wheel-load of 11.1 kN (2,500 lb).

The moving wheel-load setup used in this study did not allow wheel-loads lower than 8.9 kN (2,000 lb). However, fatigue tests under model wheel-loads of 8.9 to 11.1 kN (2,000 to 2,500 lb), which give a good indication of the fatigue strength of the bridge decks, were performed. The estimated fatigue strength in terms of the static ultimate strength and largest measured AASHTO static ultimate strength is presented in Table 2 for 1,000, 2.5 million, and 100 million wheel-load passages. The safety factors against fatigue failure for the 2.5 million wheel passage limit are presented in the same table. The fatigue strength values presented in Table 2 are estimated using an exponential expression similar to that of Equation 1 (see Figures 5 and 6). The exponential curve fitting of the experimental data points presented in Figure 5 (P versus $\log N_{pf}$) corresponds to correlation coefficients between 0.74 and 0.88. In Figure 6 (P/P_u versus $\log N_{pf}$), the exponential curve fitting corresponds to correlation coefficients between 0.92 and 0.98.

The predicted bridge deck fatigue strength level at 2.5 and 100 million wheel-load passages under a moving wheel-load is about 0.16 P_a and 0.12 P_a, respectively (see Table 2). The predicted safety factor against fatigue failure in the deck under a moving constant wheel-load for the 2.5-million wheel passage limit is about 3 to 4 for the OHBDC and the AASHTO deck design. In terms of the measured deck static ultimate strength, the 2.5-million wheel-load passage limit fatigue strength of all decks is estimated at 0.21 P_u to 0.28 P_u, which is similar to the average cracking load level of 0.26 P_u. The cracking load level corresponds to the static concentrated load reached at the end of the linear elastic region of the load-deflection response curve of a deck. If the efficiency of a deck design is determined by the number of wheel-load passages on the deck at a given moving wheel-load level (percentage of the static ultimate strength) without deck failure, the OHBDC design appears to be more efficient than the AASHTO deck design. The deck slenderness has a minor effect on the efficiency of the two deck designs with respect to their fatigue behavior.

Fatigue under moving wheel-loads results in a gridlike bottom flexural cracking (transverse and longitudinal) matching the steel reinforcement pattern (*22,23*). Initially, a major longitudinal flexural crack forms at the bottom surface of the deck along the wheel-path midway between the two adjacent steel girders supporting the deck. As the moving wheel-load causes the opening and closing of this major longitudinal crack and forces it to propagate upwards, additional longitudinal cracks appear at the bottom of the deck. The longitudinal cracks open wider and wider with an increasing number of wheel-load passages, and transverse bottom flexural cracks (perpendicular to the steel girders) also form practically at the same spacing as that of the bottom transverse flexural steel reinforcement. Although the bottom longitudinal cracks open and close (flexural mode) as the wheel-load moves back and forth on the bridge deck, the bottom transverse cracks in addition to opening and closing (flexural mode) also slide up and down (shearing mode) causing continuous rubbing of the crack interfaces. This "reversing" shear

movement of the transverse crack surfaces causes degradation of the interface shear transfer mechanism. This also results in debonding along the steel reinforcement because the cracks in both directions form usually close to the bottom steel reinforcement in a gridlike pattern.

Cracking appears to be the major reason for fatigue failure of a bridge deck subjected to a moving wheel-load. This is supported by the fact that the 2.5-million wheel-load passage limit fatigue strength of the decks under moving wheel-load is similar to the average cracking load level under a concentrated static load. Therefore, although the necessary condition for fatigue failure under stationary pulsating load is yielding of the flexural steel reinforcement, the necessary condition for fatigue failure under moving wheel-load is flexural transverse and logitudinal cracking.

Effect of Type of Loading: Pulsating versus Moving

The development of the OHBDC for deck design was based on stationary pulsating load tests conducted on 1/8-scale composite bridge deck models (*11*). The fatigue strength at 2.5 million load cycles of those bridge decks was determined to be about 0.5 P_u for the orthotropic (AASHTO) and isotropic (OHBDC) designs. These findings, based on the AASHTO design load, correspond to safety factors against fatigue failure of 8 to 10. These results are consistent with the stationary pulsating load test findings in the present research study. One major difference, however, in the two testing programs is that the tests by Batchelor et al. (*11*) were conducted on composite bridge decks, whereas the present study dealt with the response of noncomposite bridge decks.

It is known that membrane compressive action in a laterally restrained concrete bridge deck slab is the major mechanism carrying the applied concentrated load. Membrane compressive forces are induced by the restraining action of the supports and the deck region surrounding the loaded area. This deck region, however, cannot provide the same membrane action if it is damaged during fatigue. Indeed, this is what probably happens in the case of fatigue under a moving wheel-load. Every loaded section in the deck along the load path is surrounded (at least in the longitudinal direction) by damaged regions that become less and less capable of providing the membrane compressive forces that a nondamaged region could have provided. This results in a gradual transition from a two-way to a one-way slab action. The wheel-load is eventually transferred primarily in the transverse direction (perpendicular to traffic), and the bridge deck becomes a series of parallel transverse beams linked together mainly by the steel and supported on the steel girders. If the concrete bridge deck is designed to transfer most of the wheel-load in the transverse direction (AASHTO design), the transformation of the two-way deck slab action into a one-way will probably be accelerated because of the already existing orthotropy in the deck.

CONCLUSIONS

1. For a given load level, decks subjected to a stationary pulsating concentrated load exhibited much higher fatigue strength than those fatigued under a moving constant wheel-load. The stationary concentrated pulsating load tests are not adequate in predicting the fatigue strength of concrete bridge decks subjected to traffic load.
2. The estimated fatigue strength of the reinforced concrete bridge deck models under a stationary pulsating load at 2.5 million load cycles is 0.47 to 0.54 P_u (P_u = measured static ultimate strength). These values correspond to safety factors against fatigue failure of about 5 to 12 [assuming a scaled model design load of 2.3 kN (525 lb)]. The 2.5-million wheel-load passage limit fatigue strength for the bridge decks subjected to a moving constant wheel-load is estimated to be about half of their fatigue strength under a stationary pulsating load. On the basis of an exponential curve fit of the experimental fatigue data, a fatigue strength of 2.5 million is predicted to be in the range of 0.21 to 0.28 P_u. This range of fatigue strength corresponds to safety factors against fatigue failure of about 3 to 4.
3. The predicted fatigue strength of the bridge decks under a moving constant wheel-load for 2.5 million wheel-load passages is in the same range as the average flexural cracking load level of the decks of $P_{cr} = 0.26\ P_u$. The predicted fatigue strength of the decks under a moving constant wheel-load for 100 million wheel-load passages ranges from 0.14 to 0.21 P_u, which is slightly lower than the average flexural cracking load level. It appears that the fatigue design specifications should not allow flexural cracking in concrete decks. The effect of shrinkage cracking has not been studied. On the other hand, under a stationary pulsating load the fatigue strength of the decks appears to be related to the yielding load level of the decks.
4. Bridge decks subjected to a stationary pulsating load exhibited flexural radial cracking (on the bottom deck surface) similar to that observed in the static load tests. However, the cracks at the bottom surface of the bridge deck models subjected to a moving constant wheel-load formed a gridlike pattern similar to that of the bottom steel layer. On the top deck surface, longitudinal negative cracks eventually formed above the steel girders adjacent to the deck region being tested and crushing of concrete occurred along the wheelpath, especially for the higher deck slenderness and lower steel ratio.
5. For a bridge deck subjected to a moving constant wheel-load, the initial two-way deck slab action is transformed to a one-way transverse slab action as deck failure is approached. For a similar deck subjected to a stationary pulsating load of equal peak value, the initial two-way slab action is maintained until deck failure occurs, usually because of punching.
6. If the efficiency of a deck design for fatigue is determined by the number of wheel-load passages on the deck at a given moving wheel-load level ratio (P/P_u) without deck failure, the OHBDC deck design appears to be more efficient than the AASHTO design. The deck slenderness has a minor effect on the efficiency of the two designs regarding the fatigue deck behavior.

ACKNOWLEDGMENTS

This research was funded by ODOT and FHWA. Their support is greatly appreciated. Special thanks are due to Steve Marine of the Structures Laboratory, who was a major contributor in the design and construction of the wheel-load setup, and Lindberg Heat Treating Co., Solon, Ohio, for kindly donating time for the annealing of the model steel reinforcement wires.

REFERENCES

1. *Standard Specifications of Highway Bridges*, 14th ed. AASHTO, Washington, D.C., 1989.

2. Azad, A. K., M. H. Baluch, M. Y. Al-Mandil, and M. S. Al-Suwaiyan, Static and Fatigue Tests of Simulated Bridge Decks. Experimental Assessment of Performance of Bridges. *Proc., of ASCE Convention*, Boston, Mass., Oct. 1986, pp. 30–41.
3. Perdikaris, P. C., and S. R. Beim, *Design of Concrete Bridge Decks*. Final Report FHWA/OH/RR-88-004. Ohio Department of Transportation, Aug. 1988.
4. Perdikaris, P. C., S. Beim, and S. Bousias, Slab Continuity Effect on Ultimate and Fatigue Strength of R/C Bridge Deck Models. *ACI Structural Journal*, Vol. 86, No. 4, July–Aug. 1989, pp. 483–491.
5. Perdikaris, P., and M. Petrou, Code Predictions Versus Small-Scale Bridge Deck Model Test Measurements. In *Transportation Research Record, 1290*, TRB, National Research Council, Washington, D.C., 1991, pp. 179–187.
6. Petrou, M. F., and P. C. Perdikaris, Small Scale Model Tests: Arching Action in Reinforced Concrete Bridge Decks. *Proc., 3rd International Conference on Short and Medium Span Bridges*, Toronto, Ontario, Canada, Aug. 1990.
7. Petrou, M. F. *Behavior of Concrete Bridge Deck Models Subjected to Concentrated Load-OHBDC vs. AASHTO*. M.S. thesis, Case Western Reserve University, Cleveland, Ohio, May 1991.
8. Hewitt, B. E. *An Investigation of the Punching Strength of Restrained Slabs With Particular Reference to the Deck Slabs of Composite I-Beam Bridges*. Ph.D. dissertation. Queen's University at Kingston, Ontario, Canada, March 1972.
9. Hewitt, B. E., and B. deV. Batchelor. Punching Shear Strength of Restrained Slabs. ASCE *Journal of the Structural Division*, Vol. 101, ST9, Sept. 1975, pp. 1837–1853.
10. Batchelor, B. deV., and B. E. Hewitt. Are Composite Bridge Slabs Too Conservatively Designed? Fatigue Studies. *Fatigue of Concrete, ACI Special Publication SP4-15*. 1974, pp. 331–346.
11. Batchelor, B. deV., B. E. Hewitt, and P. Csagoly. An Investigation of the Fatigue Strength of Deck Slabs of Composite Steel/Concrete Bridges. In *Transportation Research Record 664*, TRB, National Research Council, Washington, D.C., 1978, pp. 153–161.
12. Fang, I-K. Behavior of OHBDC-Type Bridge Deck on Steel Girders. Ph.D. dissertation. University of Texas at Austin, Dec. 1985.
13. Fang, I-K., J. Worley, N. H. Burns, and R. E. Klingner. Behavior of Isotropic R/C Bridge Decks on Steel Girders. ASCE *Journal of Structural Engineering*, Vol. 116, No. 3, March 1990, pp. 659–678.
14. Perdikaris, P. C., and S. Beim. RC Bridge Decks Under Pulsating and Moving Load. ASCE *Journal of Structural Engineering*, Vol. 114, No. 3, March 1988, pp. 591–607.
15. Wang, A. Fatigue Behavior of Small-Scale R/C Bridge Decks Subjected to Pulsating and Moving Loads. M.S. thesis. Case Western Reserve University, Cleveland, Ohio, May 1992.
16. *Ontario Highway Bridge Design Code*, 2nd ed. Ontario Ministry of Transportation and Communications, Downsview, Canada, 1983.
17. Okada, K., H. Okamura, and K. Sonoda. Fatigue Failure Mechanism of Reinforced Concrete Bridge Deck Slabs. In *Transportation Research Record 664*, TRB, National Research Council, Washington, D.C., 1978, pp. 136–144.
18. Sonoda, K., and T. Horikawa. Fatigue Strength of Reinforced Concrete Slabs Under Moving Loads. *Proc., IABSE Colloquium, Fatigue of Steel and Concrete Structures*, Vol. 37, Lausanne, Switzerland, 1982, pp. 455–462.
19. Hayashi, H., M. Okino, S. Matsui, and K. Sonoda. Reliability of a Repairing Method for Cracked and Damaged RC Slabs of Bridge Deck. *Proc., Pacific Concrete Conference*, New Zealand, Nov. 8–11, 1988, pp. 613–624.
20. Tanihira, T., K. Sonoda, T. Horikawa, and H. Kitoh. Low Cycle Fatigue Characteristics of Bridge Deck RC Slabs Under the Repetition of wheel-loads. *Proc., Pacific Concrete Conference*, New Zealand, Nov. 8–11, 1988, pp. 381–392.
21. Sabnis, G. M., H. G. Harris, R. N. White, and M. Mirza. *Structural Modeling and Experimental Techniques*, Prentice-Hall, Englewood Cliffs, N.J., 1983.
22. Petrou, M. F. *Fatigue Performance of AASHTO and OHBDC Design for Non-Composite Reinforced Concrete Bridge Decks*. Ph.D. dissertation. Case Western Reserve University, Cleveland, Ohio, Aug. 1993.
23. Perdikaris, P. C., M. F. Petrou, and A. Wang. *Fatigue Strength and Stiffness of Reinforced Concrete Bridge Decks*. Final Report FHWA/OH-93/016. Ohio Department of Transportation, March 1993.

The contents of this paper reflect the views of the authors, who are responsible for the findings and conclusions presented herein, and do not necessarily reflect the views of ODOT or FHWA.

Publication of this paper sponsored by Committee on Dynamics and Field Testing of Bridges.